JOINT INSTITUTE FOR NUCLEAR RESEARCH, DUBNA

PREPRINT P9 - 5558

EXPERIMENTS IN α-PARTICLE ACCELERATION BY THE COLLECTIVE METHOD

V.P. Sarantsev, V.P. Rashevskij, A.K. Kaminskij,
V.I. Mironov, V.P. Fartushnyj, A.P. Sergeev,
V.G. Novikov, S.I. Tyutyunnikov, A.M. Kaminskaya

(Submitted to JETP Letters)

Dubna, 7 January 1971

Translated at CERN by R. Luther
Revised by N. Mouravieff
(Original : Russian)

(CERN Trans. 71-1)

Geneva
(January 1971)

In 1956, V.I. Veksler$^{1)}$ indicated the possibility of performing new methods of acceleration involving the use of collective interactions. During the past few years these ideas have been successfully developed on both theoretical and experimental levels, firstly in the USSR$^{2)}$ and later in other countries.

The staff of the JINR Department for New Acceleration Methods has made great progress in the development of the collective acceleration technique, and has accelerated α particles on a collective linear ion accelerator model. This gave experimental proof that the new acceleration method is efficient.

In order to accelerate protons or heavy ions by the new method, a dense cluster of electrons is required. In the JINR collective ion accelerator model, a ring-shaped bunch of electrons rotating in a magnetic field is used to form this cluster. The LIU-3000 induction linac is used to inject the electrons. The 100 A, 1.5 MeV beam is injected into the adhesator's weak-focusing field to a radius of 40 cm. The pulse fields are switched on to ensure pinching of the beam and further adiabatic compression down to a radius of 6 cm. During the initial turns, the beam has an elliptical cross-section with semiaxes $A_r \sim 1.6$ cm in the radial direction and 1.2 cm in the axial. During adiabatic compression, the beam's transverse dimensions are reduced$^{3)}$.

Calculations show that, allowing for variations in the frequency of betatron oscillations due to the capture of ions from the helium medium in which compression occurs, the ring's cross-section measures $\sim$ 1 mm at the final stage of compression when $P = 10^{-7}$ mm Hg. These calculations are confirmed by the measurements made of the ring's radial cross-section during its ejection from the potential well. Figures 5 and 6 illustrate the adhesator's system of coils and the magnetic field produced by this system. As can be seen from these figures, in order to eject and accelerate the ring, the magnetic barrier must be distorted adiabatically -- its symmetry must be disturbed in such a way that an ejecting force acts on the cluster in the z direction. To do this, coils (4), (5), and (6) are shunted at a specific moment by means of the spark gap (9). As a result, a magnetic field is set up in the adhesator (a graph of this field is also shown in Fig. 6), the axial gradient of which creates the required accelerating force. The problem of confining the ions within the ring of electrons during acceleration imposes specific demands on the field gradient[4]. The gradient is controlled by selecting the time for switching on the spark gap (9) and solenoid (7). It is hard to measure local gradient values very accurately. Therefore, when the ring was accelerated, the mean field gradient in the 40 cm accelerating area was maintained at approximately 10 Oe/cm. With this gradient, the ring is not accelerated to the maximum, and doubly-charged α particles can be accelerated to 30 MeV. As calculations show[4], the ratio of the number of accelerated α particles to those initially trapped in the potential well is 30%.

The accelerated ring, charged with α particles, strikes the target which is made from copper foil. The target is located in the region of strong field decay; a dummy target is placed directly in front of the target and the electron component is precipitated on this. However, due to the irregular precipitation of the electron ring, the energy of the α particles is spread out towards the higher energies.

A technique of measuring the induced activity on the copper target was used to monitor the beam of α particles and determine its main parameters. This activity is the result of the interaction of accelerated α particles with the nuclei of ^{63}Cu and ^{65}Cu. The main nuclear reactions occurring on the copper are the following:

$^{63}\mathrm{Cu}(\alpha,n)^{66}\mathrm{Ga}$ $T_{1/2}$ = 9.4 hrs
$^{63}\mathrm{Cu}(\alpha,2n)^{65}\mathrm{Ga}$ $T_{1/2}$ = 15 min
$^{65}\mathrm{Cu}(\alpha,n)^{68}\mathrm{Ga}$ $T_{1/2}$ = 70 min
$^{65}\mathrm{Cu}(\alpha,2n)^{67}\mathrm{Ga}$ $T_{1/2}$ = 78 hrs.

^{66}Ga is a very convenient isotope for monitoring gamma radiation as its gamma spectrum contains two intense lines of 511 keV and 1040 keV. As the measurements were made 4-5 hours after irradiation, the contribution from the reaction's other channels in the 511 keV line is insignificant due to the short half-life of ^{68}Ga and ^{65}Ga [5].

The bremsstrahlung interaction of the electrons with the nuclei of ^{63}Cu and ^{65}Cu forms a secondary reaction on the copper. The photonuclear reaction threshold on $^{65}\mathrm{Cu}(\alpha,n)$ is 11 MeV. In order to estimate the effect of isotope yield from these reactions, the copper target was irradiated by the ring of electrons at maximum compression. There is no activity in the gamma spectrum for this target in the energy ranges which interest us. Thus, by measuring gamma spectra from the copper foil, it is possible to assess the energy and number of α particles striking the target.

Estimates were made of the efficiency with which the α particles are recorded using this isotope. It was shown that it is possible to monitor α-particle fluxes with $N_\alpha > 5 \times 10^8$ and $E_\alpha > 10$ MeV.

To determine the parameters of the α-particle beam, targets were placed 40 cm from the median plane. The target is a composite type comprising five sheets of copper and aluminium foil. The gauge of the copper foil and aluminium foil is 12 mg/cm^2 and 5.4 mg/cm^2, respectively. Four to five hours after irradiation, the activity of the foil was measured on a scintillation spectrometer. Figure 1 shows the full gamma spectrum, Figs. 2 to 4 show the spectrometer's main parameters, the energy dependence of γ-quanta recording efficiency, and the calibration line.

The gamma spectrum contains two lines of 511 keV and 1040 keV. The half-life of this activity was measured giving a value of $T_{1/2} = 9$ hrs. The energy was measured by measuring the activity in each layer. The results are shown in Fig. 7. It can be seen that the maximum yield occurs on sheet 4 of the copper foil. The energy of the incident α particles was estimated using the results from papers$^{6,7)}$, and also those obtained by irradiating the same foil stack in the U-200 cyclotron at the Laboratory for Nuclear Reactions. These estimates give the value $E_\alpha = (29 \pm 6)$MeV.

The error in determining the energy value depends on the error in measuring the thickness of the copper foil, which amounts to 10%, and the inaccuracy in fixing the position of the maximum in the excitation function.

Knowing the energy of the α particles, the integrated flux of incident α particles can be determined according to the isotope yield on foil 4 using the formula

$$N_\alpha = \frac{N_0}{\sigma(\alpha,n)\ N_{nuc}} \tag{1}$$

where N_0 is the number of active ^{66}Ga nuclei at the initial time and N_{nuc} is the number of target nuclei per 1 cm^2;

$$N_0 = \frac{S_{peak} \cdot e^{\lambda t_{delay}}}{\kappa \cdot \varepsilon(1 - e^{-\lambda t_{meas}})} \tag{2}$$

S_{peak} - area for photopeaks

κ - absolute quantum yield

ε - efficiency of quantum recording

t_{delay} - time between end of irradiation and beginning of measurement

t_{meas} - measuring time

λ - ^{66}Ga decay constant.

The calculations give the value for the integrated flux of α particles as $N_\alpha \simeq 5 \times 10^9$.

The error in determining the number of α particles depends mainly on the error in measuring the energy of the α particles (20%) and the thickness of the copper target (10%). Thus the flux of α particles is fixed at

$$N_\alpha = (5 \pm 1.5) \times 10^9 \quad .$$

The experiments and measurements have indicated the presence of accelerated α particles and have thus proved unambiguously that it is intrinsically possible to perform acceleration using the collective method.

In conclusion, the authors wish to thank all those colleagues in the department who helped with the experiments and assessment of results, in particular: A.A. Rashevskaya, V.S. Khabarov, I.V. Kozhukhov, I.N. Ivanov, E.A. Perel'shtejn, N.B. Rubin, V.A. Prejzendorf, and also Yu.Ts. Oganesyan and A.T. Shamsutdinov from the Laboratory for Nuclear Reactions.

BIBLIOGRAPHY

1a) V.I. Veksler, Principle of acceleration of charged particles, CERN Symposium, Vol. 1, p. 80 (1956).

1b) V.I. Veksler, Coherent principle for the acceleration of charged particles, Atomnaya Energiya 5, 427 (1957).

2a) V.I. Veksler, V.P. Sarantsev et al., Collective linear acceleration of ions, JINR preprint P-9-3440, Dubna (1968).

2b) V.I. Veksler et al., Collective linear acceleration of ions, Proc. 6th Int. Conf. on High-Energy Accelerators, Cambridge (1967), p. 289.

3) I.N. Ivanov, M.L. Iovnovich, A.B. Kuznetsov, Yu.L. Obukhov, K.A. Reshetnikova, H.B. Rubin, V.P. Sarantsev and O.I. Yarkovoj, Problems of particle motion in the adhesator, JINR preprint P-9-4132, Dubna (1968).

4) I.N. Ivanov, E.A. Perel'shtejn and V.P. Sarantsev, On the problem of accelerating ions by means of a ring-shaped bunch of electrons in a decaying magnetic field, Report to the 11th All-Union Conference on Charged Particle Accelerators, Moscow (1970).

5) Table of Isotopes, 1968.

6) Phys. Rev. 116, No. 5, 1193 (1959).

7) Northcliffe, Nuclear Data Tables, Section A, v.7, N 3-4 (1970).

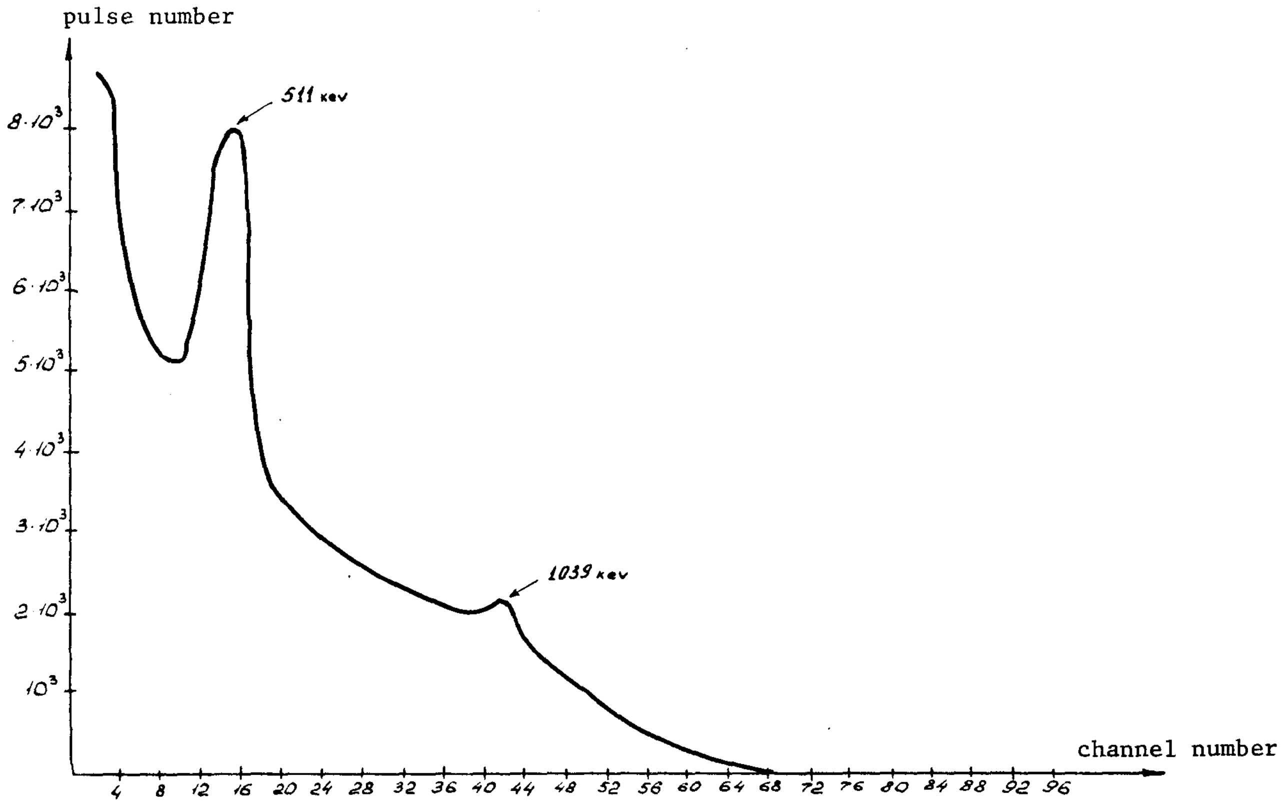
pulse number
8·10³
7·10³
6·10³
5·10³
4·10³
3·10³
2·10³
10³
511 kev
1039 kev
channel number
4
8
12
16
20
24
28
32
36
40
44
48
52
56
60
64
68
72
76
80
84
88
92
96

Fig. 1

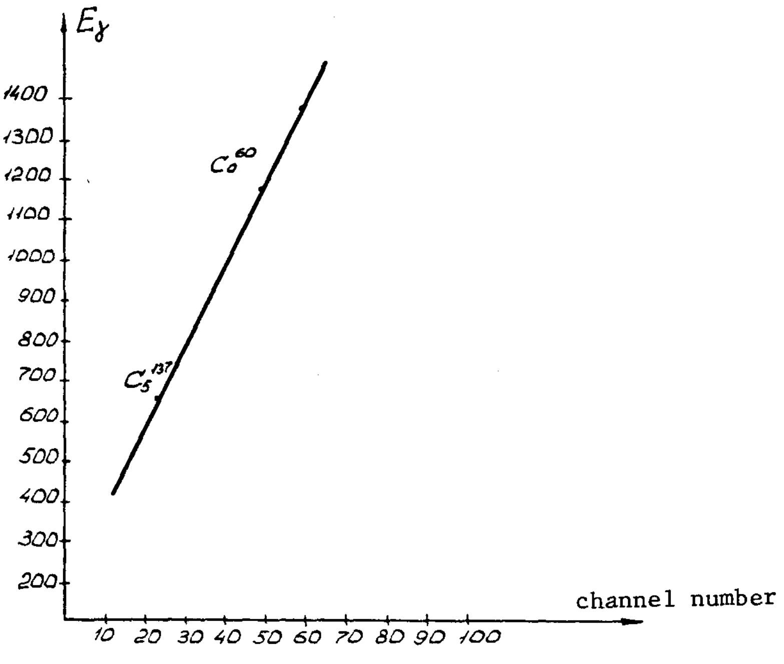
Eγ
1400
1300
1200
1100
1000
900
800
700
600
500
400
300
200
Co⁶⁰
Cs¹³⁷
channel number
10
20
30
40
50
60
70
80
90
100

Fig. 2

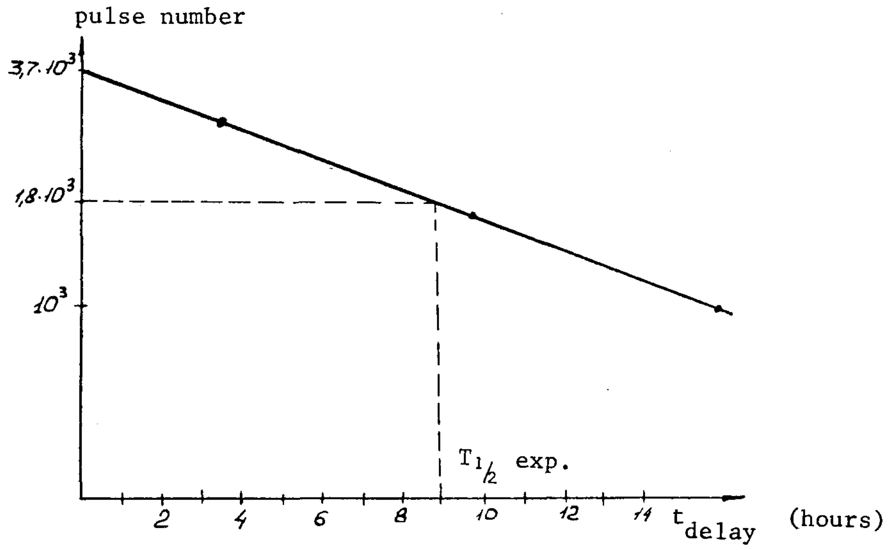
pulse number
3,7·10³
1,8·10³
10³
T1/2 exp.
2
4
6
8
10
12
14
t delay
(hours)

Fig. 3

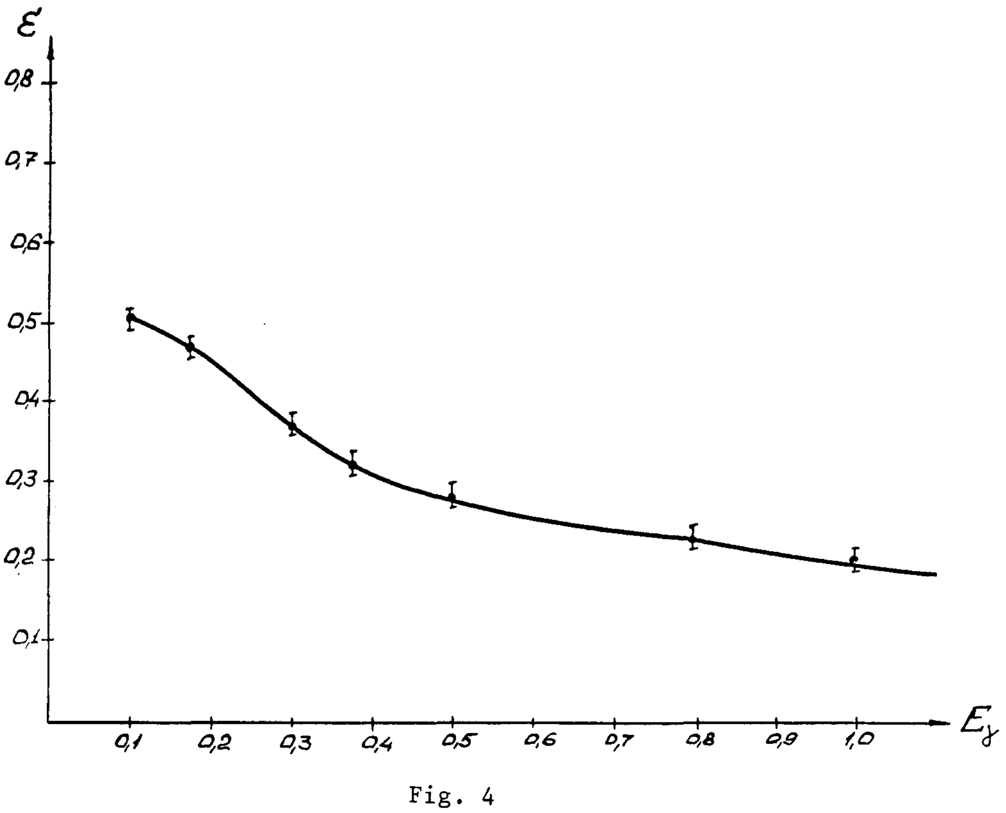
ε
0,8
0,7
0,6
0,5
0,4
0,3
0,2
0,1
0,1
0,2
0,3
0,4
0,5
0,6
0,7
0,8
0,9
1,0
Eγ

Fig. 4

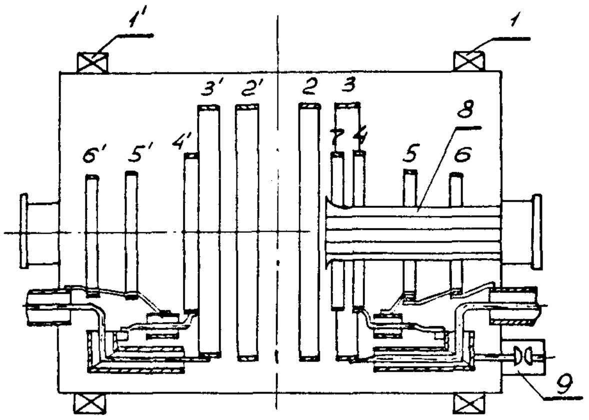

Fig. 5

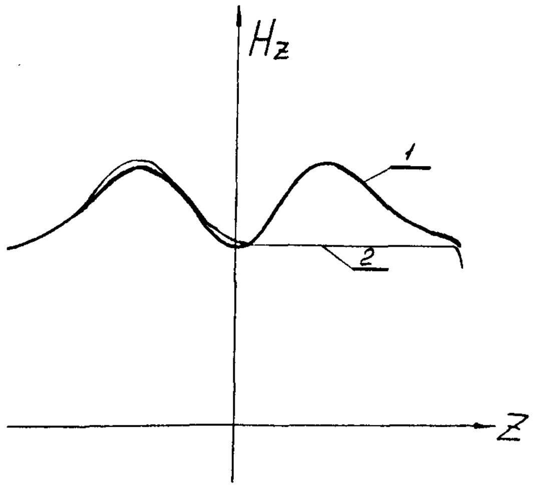

Fig. 6

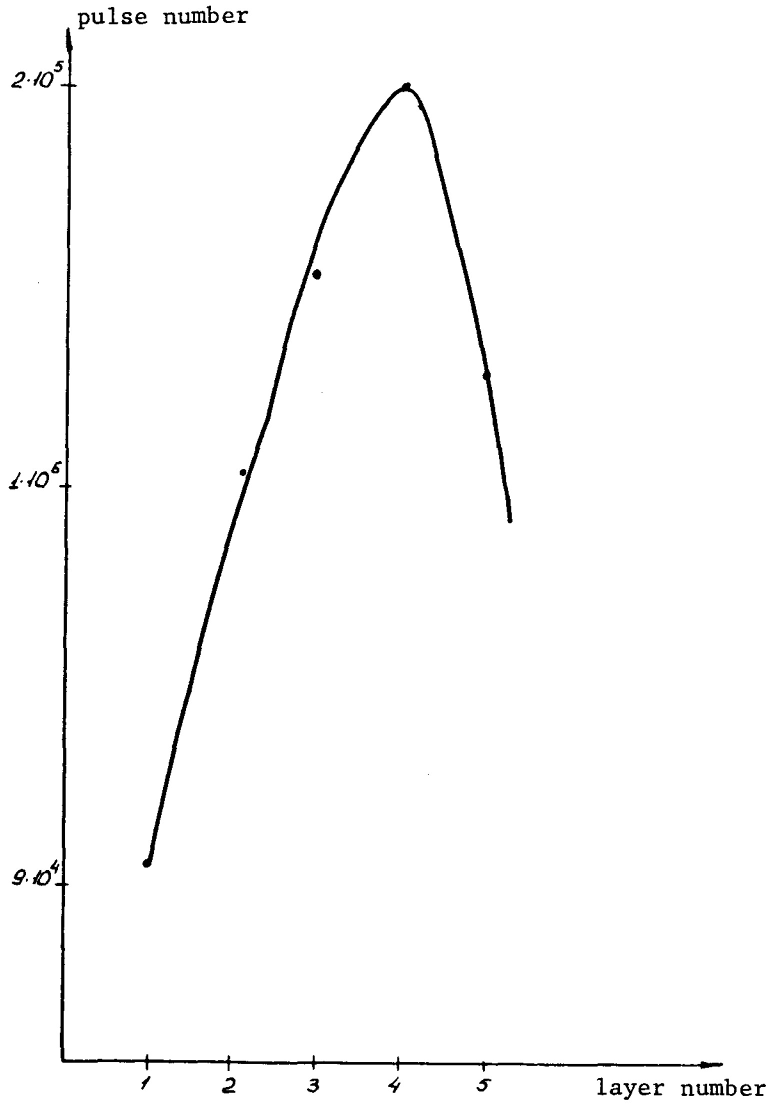

Fig. 7